



Cite this: DOI: 10.1039/c7lc00768j

## An advanced selective liquid-metal plating technique for stretchable biosensor applications†

Guangyong Li<sup>ab</sup> and Dong-Weon Lee  <sup>\*b</sup>

This paper presents a novel stretchable pulse sensor fabricated by a selective liquid-metal plating process (SLMP), which can conveniently attach to the human skin and monitor the patient's heartbeat. The liquid metal-based stretchable pulse sensor consists of polydimethylsiloxane (PDMS) thin films and liquid metal functional circuits with electronic elements that are embedded into the PDMS substrate. In order to verify the utility of the fabrication process, various complex liquid-metal patterns are achieved by using the selective wetting behavior of the reduced liquid metal on the Cu patterns of the PDMS substrate. The smallest liquid-metal pattern is approximately 2  $\mu\text{m}$  in width with a uniform surface. After verification, a transparent flowing LED light with programmed circuits is realized and exhibits stable mechanical and electrical properties under various deformations (bending, twisting and stretching). Finally, based on SLMP, a wireless pulse measurement system is developed which is composed of the liquid metal-based stretchable pulse sensor, a Bluetooth module, an Arduino development board, a laptop computer and a self-programmed visualized software program. The experimental results reveal that the portable non-invasive pulse sensor has the potential to reduce costs, simplify biomedical diagnostic procedures and help patients to improve their life in the future.

Received 22nd July 2017,  
 Accepted 22nd August 2017

DOI: 10.1039/c7lc00768j

rsc.li/loc

## Introduction

Monitoring vital signs is an effective way for physicians to assess the status of the essential functions of the human body in modern medical care and diagnosis.<sup>1</sup> These physiological signals in the biological system can be accurately monitored and recorded using various medical systems.<sup>2,3</sup> In general, the real-time monitoring process of vital signals is complex and requires experienced personnel. Sensors employed in current systems also show limited flexibility and stretchability when they are mounted on human bodies. Traditional monitoring techniques have several advantages in early diagnosis for patients, but are limited compared to those widely used due to the high mechanical stiffness of the sensors. With attractive properties such as biocompatibility, light weight and transparency, the development of stretchable sensors that monitor the changes in vital signs of human beings such as temperature, blood pressure, breathing rate, *etc.* has received great interest from the scientific community.<sup>4</sup> In recent years, a variety of innovative manufacturing technologies have been

developed to meet market requirements in stretchable electronics. These sensors are integrated with tiny electronic components that can be adhered onto the non-planar skin of humans.<sup>5–13</sup> In the early stages of the development for flexible electronics, thin films patterned with deterministic geometries or conductive particles in elastomer have been widely used to minimize changes in electrical properties.<sup>11–13</sup> Although these techniques are very suitable for flexible electronics, it is not easy to apply them to stretchable electronics.<sup>10</sup> Compared to other methods, liquid metals can only be categorized as intrinsically stretchable because they are softer than common materials used for flexible electronics. The most efficient technology for stretchable electronics is to print liquid metals on an elastomeric substrate. Various liquid-metal printing techniques such as stencil mask-based printing,<sup>14,15</sup> injecting,<sup>16–20</sup> atomized spraying,<sup>21–23</sup> direct writing,<sup>24–29</sup> masked deposition,<sup>30</sup> and inkjet printing<sup>31</sup> have been developed to realize flexible and stretchable electronics. For the injecting technique, the microfluidic channel injected with liquid metal can be utilized as the electrical interconnector in the applications of stretchable RF radiation sensors, capacitors, inductors and liquid metal-based electrical interconnectors.<sup>16–20</sup> The resolution of liquid metal patterns fabricated by the injecting technique depends on the resolution of the microfluidic channel. The max strain of liquid metal-based electrical interconnectors can be up to ~600%.<sup>20</sup> Nevertheless, when the size of the microfluidic channel is

<sup>a</sup> Faculty of Mechanical Engineering and Mechanics, Ningbo University, Ningbo, 315211, China

<sup>b</sup> MEMS and Nanotechnology Laboratory, School of Mechanical Engineering, Chonnam National University, Gwangju, 61186, South Korea.

E-mail: [mems@chonnam.ac.kr](mailto:mems@chonnam.ac.kr); Fax: +82 62 5301684; Tel: +82 62 5301689

† Electronic supplementary information (ESI) available. See DOI: 10.1039/c7lc00768j

decreased to below 20  $\mu\text{m}$ , the oxidized liquid metal is difficult to inject into the nozzle. Due to the extra demand for a needle and syringe for liquid metal injecting, this manual method has some drawbacks in geometry and high-volume manufacturing. For the other techniques mentioned above, the low resolution (pattern planar dimension  $>100\ \mu\text{m}$ ) and irregular edge of printed liquid metal patterns provide limits to the demands of stretchable electronics. A lift-off technique is also applied to liquid metals by spreading the metal onto substrates covered by photoresist patterns and then dissolving away the photoresist, leaving behind only the liquid metal in contact with the substrate. This technique allows the formation of liquid metal patterns with about 20  $\mu\text{m}$  features. Even though a variety of excellent methods have been developed, the technology for reliably forming liquid metal patterns of several micrometers in a large area still remains a challenge. The biocompatibility of stretchable sensors is also one of the important considerations in design and fabrication processes.

Herein, we developed a stretchable biosensor platform (liquid metal-based stretchable pulse sensor) that uses an advanced selective-liquid metal plating (SLMP) process to enable comfortable monitoring of a patient's condition for personal healthcare. The SLMP process is mainly based on the selective wetting behaviour of hydrochloric acid (HCl)-treated Galinstan (gallium-indium-tin liquid alloy) on various thin film surfaces. To summarize briefly, the reduced Galinstan droplets are in contact with the metal patterns (Au/Cr patterns) and the polydimethylsiloxane (PDMS) substrate, respectively, exhibiting superlyophilic and superlyophobic characteristics (described in Fig. S1 of the ESI†). The superlyophilic characteristic of metal materials allows the selective plating of Galinstan on the metal-patterned PDMS surface. However, the corrosion of a thin Cr layer on the HCl-treated Galinstan greatly affects the uniformity of the liquid-metal patterns and this restricts the high resolution (shown in Fig. S2 of the ESI†). More details of the SLMP process have been discussed in our previous works.<sup>32–36</sup> In order to improve the uniformity and avoid the corrosion issue between the Cr layer and the HCl-treated Galinstan, the Au/Cr patterns are covered with a Cu thin layer. This is because HCl acid does not react with Cu. Only metals whose standard reduction potential is lower than the standard reduction potential of hydrogen react with non-oxidizing acids such as HCl and diluted  $\text{H}_2\text{SO}_4$  to displace hydrogen. As a result, the minimum line width that can be realized is greatly improved.

## Results and discussion

### Principle of the liquid-metal-based stretchable pulse sensor

In modern medical treatment and diagnosis, several methods such as electrocardiography (ECG), photoplethysmography (PPG), *etc.* have been developed for measuring the heart rate. Of these heart rate monitoring methods, ECG is widely used as a standard diagnostic technique. However, the ECG technique requires specialized equipment and has diagnostic lim-

itations that restrict the patient's activities. This method also causes discomfort from the physiological and psychological points of view. The PPG technique is a non-invasive, inexpensive, reliable and low power consuming optical technique that makes it easier to monitor a patient's pulse compared to ECG. In the PPG technique, the pulse rate can be easily monitored from the change in the transmittance induced by blood pressure when the light from a light-emitting diode (LED) illuminates the human skin. However, limited flexibility and stretchability remain as drawbacks of the PPG technique. Therefore, we proposed a new method of fabricating a flexible pulse sensor based on liquid metal, as shown in Fig. 1, by combining the principle of PPG and the improved SLMP technology. The pulse sensor is a kind of reflection-type photoelectric sensor which is composed of a light source (LED) and a photoelectric converter (schematic diagram shown in Fig. S3 of the ESI†). Because arterial blood oxygen and hemoglobin are sensitive to light in the wavelength range of 500 nm to 700 nm, a green LED with a wavelength of about 560 nm is used as the light source. During each cardiac cycle, the green light illuminates the blood vessel under the skin of a person and the blood volume in the arterial blood vessels changes periodically, causing a change in the transmittance. The reflected light from blood vessel cells is measured using a photo sensor and converted to electrical signals with the help of a photoelectric converter (model: APDS-9008). To avoid any influence from environmental noise, a low-pass filter and an operational amplifier (model: MCP6001) are integrated with the stretchable biosensor platform.

### Liquid-metal pattern embedded in PDMS

In order to verify the applicability of the improved SLMP technique for stretchable or flexible electronics, various liquid-metal patterns with different widths and gap distances are demonstrated as shown in Fig. 2. As can be seen in Fig. 2(a), the first test pattern includes liquid-metal lines with a width in the range of 2  $\mu\text{m}$  to 100  $\mu\text{m}$  on the substrate. Each liquid-metal line is spaced with an edge-to-edge separation of 50  $\mu\text{m}$ . Next, liquid-metal lines having a line width of 50  $\mu\text{m}$  are formed on the substrate as shown in Fig. 2(b). The edge-to-edge separations in the line arrays are in the range of 2  $\mu\text{m}$  to 100  $\mu\text{m}$ . As mentioned in our previous works,<sup>36</sup> the concentrations of HCl solutions and the rolling time of the reduced liquid-metal over the metal patterns significantly affect the uniformity of the liquid-metal pattern, especially the edge of the patterns. This is due to the chemical reaction between diluted-HCl and thin Cr patterns (shown in Fig. S2a1, b1 and c1 of the ESI†). This can be improved by changing the existing SLMP process. The uniform liquid-metal patterns fabricated using the improved SLMP technique show better pattern edges, even for the smaller liquid-metal lines with a width of 2  $\mu\text{m}$  (shown in Fig. S2a2, b2 and c2 of the ESI†).

Fig. 3(a and b) show microscale alphabet letters and micro-flower patterns successfully generated on a silicon

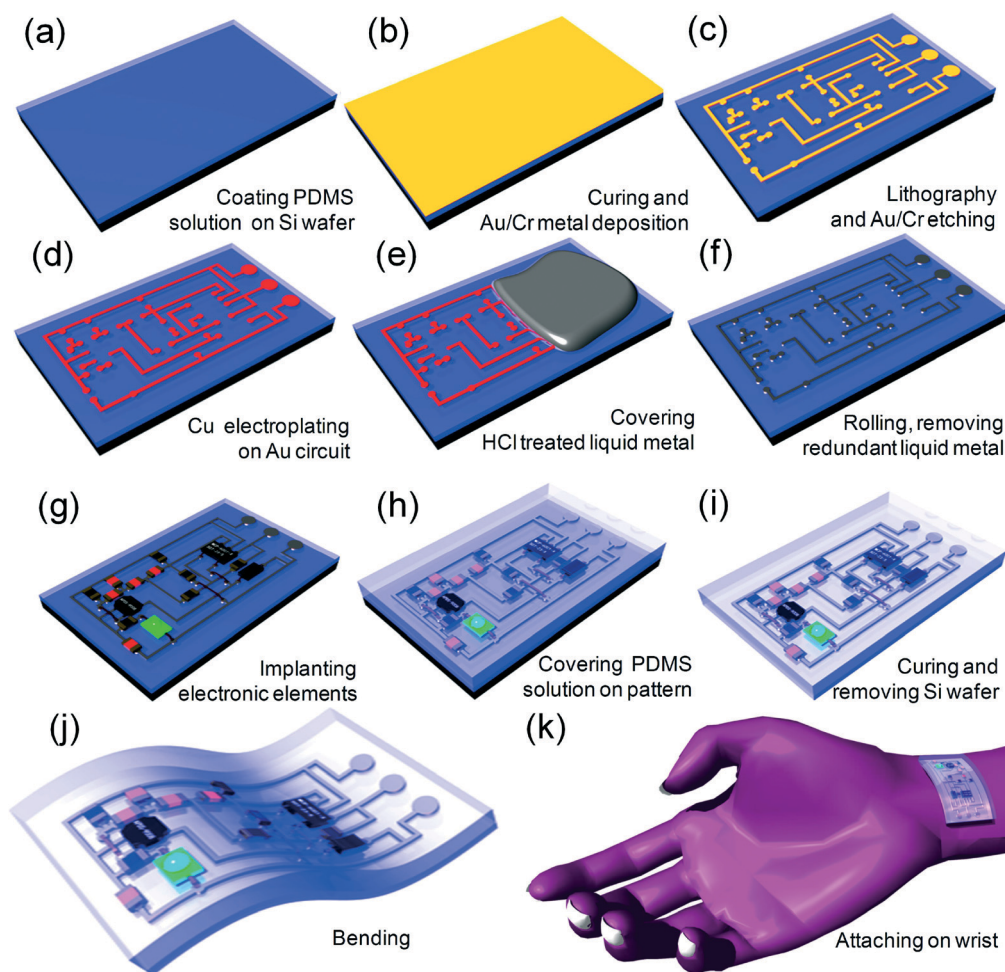


**Fig. 1** Fabrication process of the liquid-metal-based stretchable pulse sensor, (a) Spin-coating of PDMS solution onto a Si wafer. (b) PDMS curing, oxygen plasma treatment, and Au/Cr (100 nm/10 nm) deposition using an electron-beam (e-beam) evaporator. (c) Photolithography and Au/Cr etching. (d) Cu electroplating (2  $\mu\text{m}$ ) on the Au pattern. (e) Dropping HCl-treated liquid-metal onto the adhesion patterns. (f) Rolling of the liquid-metal droplet over the PDMS substrate and removing the excess liquid-metal droplet. (g) Implanting electronic elements on the liquid-metal circuit. (h) Covering the liquid-metal pattern with a PDMS solution. (i) PDMS curing and separation of the Si wafer. (j) Bending test. (k) Attaching the circuit onto the wrist.

dioxide surface. This method ensures the improved uniformity of the liquid metal pattern edge even at different sizes. The minimum width of the liquid-metal patterns is less than 2  $\mu\text{m}$ . The complex liquid metal patterns are embedded in a PDMS film which includes Chinese characters and dragon patterns as shown in Fig. 3(c–f), demonstrating the versatility of the approach to rapidly fabricate liquid-metal-patterns with a milli-to-microscale resolution over a large area. The liquid metal-based complex circuit embedded in the PDMS thin film (with a 600  $\mu\text{m}$  thickness) can be bent or stretched arbitrarily when attached to the human skin (Fig. 3(c–k)). In addition, the transparency of the flexible sensor exceeds 95% in the visible light range. Although the circuit made of liquid metal embedded in the PDMS is not transparent, it almost has no influence on the transparency of the flexible electronics when the line width of the circuit is  $<100 \mu\text{m}$ .<sup>36</sup> The stretchability can be easily improved by employing Ecoflex (a platinum-catalyzed silicone rubber) as a substrate.

### Application of the liquid-metal-based stretchable pulse sensor

After demonstrating the functionalities of the improved SLMP technique, we realized its practicality by implementing transparent LED circuits, as shown in Fig. 5(a–d). The fabrication processes of the LED circuit are similar to those of the pulse sensor except for the integrated electronic elements. As discussed in earlier works,<sup>36</sup> the change in resistance of the stretchable liquid-metal wires seriously affect the electrical characteristics of the sensor when the width of the liquid-metal lines is less than 50  $\mu\text{m}$ . If the wire width is greater than 50  $\mu\text{m}$ , the resistance change can be ignored even after 100% stretching. In order to maintain the stable electrical performance for stretchable electronics, we applied “S”-shaped liquid-metal wires instead of straight lines during the fabrication. The resistance change of the S-shaped liquid-metal wire (wire width: 5  $\mu\text{m}$ , straight length: 10 mm) is less



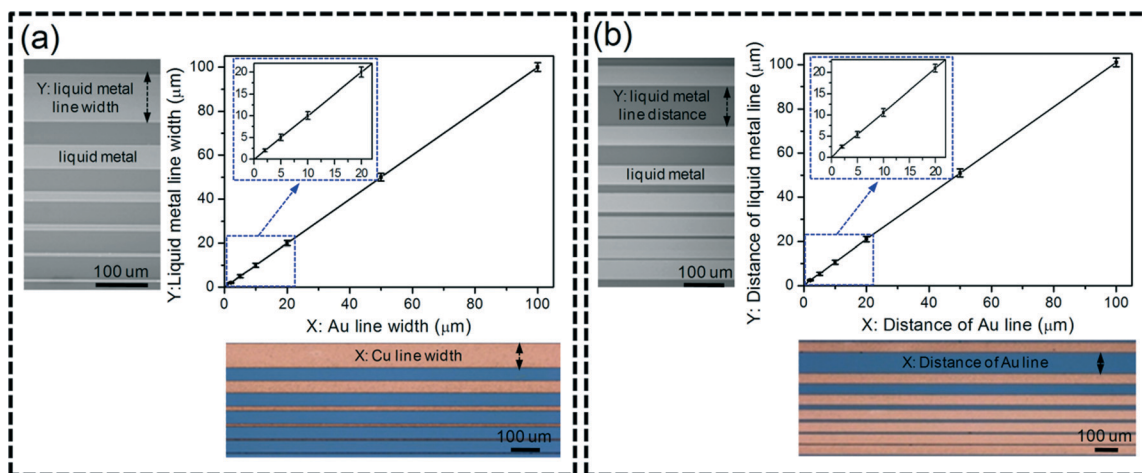


Fig. 2 SEM and optical images of liquid-metal; the plots of (a) the width of the liquid-metal lines versus the width of the Cu lines, and (b) the length of the liquid-metal lines versus the length of the Cu lines before liquid-metal plating. The width and length of liquid-metal lines vary in the range from 2  $\mu\text{m}$  to 100  $\mu\text{m}$ .

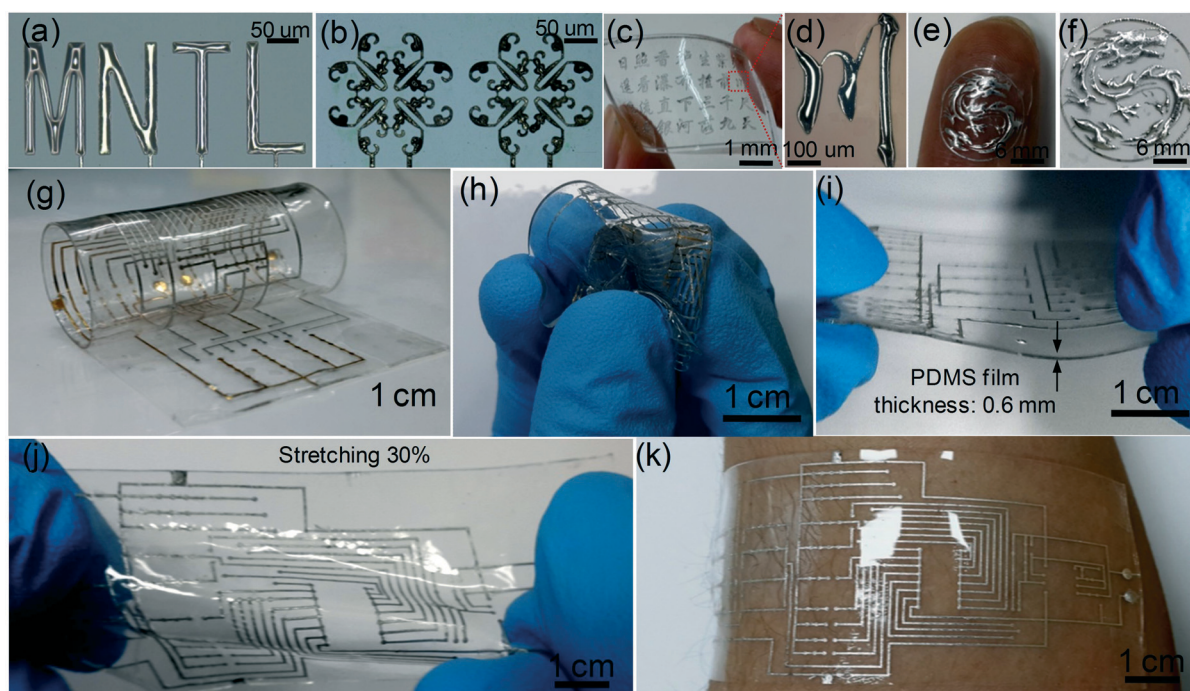


Fig. 3 Complex patterns of liquid-metal plated on a silicon dioxide surface and embedded in PDMS with different patterns: (a) microscale alphabet letters, (b) flower, (c and d) Chinese characters, and (e and f) dragon. Complex liquid-metal circuit embedded in the thin PDMS film with (g) crimping and (h) crumpling deformation, (i) 600  $\mu\text{m}$ -thickness, and (j) stretching deformation. (k) The circuit attached onto the skin of the arm for demonstration.

than 30% after 100% stretching as shown in Fig. 4. In addition, the stretchable circuit can be self-healed electrically under ambient conditions when they are damaged by something sharp. This is due to the liquid characteristics of the electrical wires.

Fig. 5(a) shows an example of stretchable electronic platforms using the advanced SLMP method. To simplify the fabrication process, we employed an embedded liquid-metal wire with a wire width of 300  $\mu\text{m}$  connected to electronic de-

vices in the process of manufacturing the stretchable electronics. The LED circuit consists of an oscillator chip (NE555), a counter chip (CD40174), LED lights, diodes, resistors, and capacitors (circuit diagram shown in Fig. S4 of the ESI†). Fig. 5(b–d) reveal that the fabricated LED circuits are optically transparent, and exhibit excellent electrical and mechanical behaviors under arbitrary deformations. Moreover, it can be easily attached to the human skin thanks to the soft-elastic characteristics of the PDMS material. An

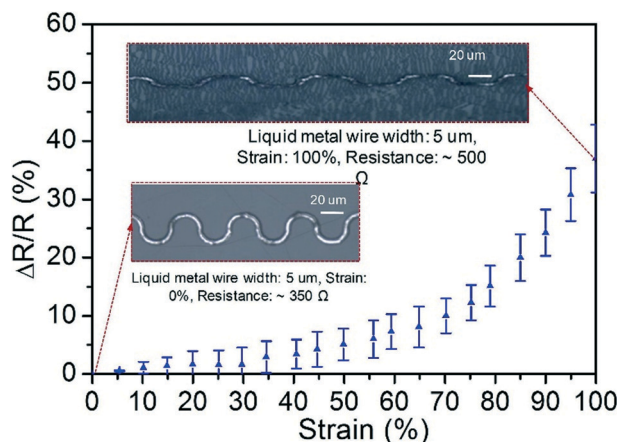


Fig. 4 Electrical characterization of the liquid-metal wire with an “S” shape (wire width: 5  $\mu\text{m}$ , straight length: 10 mm).

additional decrease in the wire line width can be easily achieved by utilizing the aforementioned “S”-shaped patterns.

Finally, the improved SLMP technique is employed to fabricate the stretchable pulse sensor for personal health monitoring applications. After applying a 5 V DC power, the green LED light is turned on, and the stretchable pulse sensor works very well under arbitrary deformations (Fig. 5(e–g)). Fig. 5(h–j) show optical images of the fabricated stretchable pulse sensor attached to various areas of the human skin such as the finger, earlobe, and wrist. For non-invasive heart-rate monitoring in home health care, the stretchable pulse sensor is combined with a home-made wireless system. The wireless healthcare system consists of the fabricated pulse sensor, a Bluetooth module, an Arduino board, a laptop computer and a home-made graphic user interface (GUI) (Fig. 5(k and l)). When the stretchable pulse sensor is attached to a person's skin, the electrical signal obtained from the sensor is converted to a digital signal using the Arduino board with a Bluetooth module. The digital signal is wirelessly transmitted to the laptop computer and then the results are displayed on the monitor (Video SV. 1 and SV. 2 of the ESI†). Fig. 5(m–q) show the experimental results of the stretchable pulse sensor attached to the human skin. The attached pulse sensor showed stable performance even under various mechanical stimulations such as torsion, stretching, *etc.* The pulse period also increased with the increase of the exercise intensity, and the pulse shape and cycle were successfully visualized through the home-made GUI. These experimental results reveal that the stretchable pulse sensor exhibits excellent electrical and mechanical behaviors in any mechanical strain such as flexure, torsion, and stretching.

## Conclusion

In this paper, a liquid-metal-based flexible and stretchable pulse sensor realized using an advanced SLMP technique has been introduced for personal healthcare applications. The

fabricated pulse sensor fully covers the human skin and monitors the patient's heartbeat in a simple and inexpensive way that is suitable for home healthcare. The proposed SLMP technique has significantly improved the resolution and the uniformity of liquid-metal patterns with a minimum width of about 2  $\mu\text{m}$ . After optimization of the fabrication processes, we verified the applicability of the advanced SLMP technique by realizing a transparent LED light with programmed circuits. Finally, the idea is utilized to realize the platform of the liquid-metal-based pulse sensor (integrated with a light source, a photoelectric converter, a low-pass filter, and an operational amplifier). The observed results reveal that the proposed pulse-measurement system is very convenient and comfortable for monitoring patients' heart rate. We believe that the portable non-invasive liquid-metal-based stretchable pulse sensor has great potential to improve the life of patients.

## Experimental section

### Preparation of liquid-metal

Galinstan is a commercially available (from Geratherm Medical AG, Germany) eutectic GaInSn metal alloy (68.5%, 21.5%, and 10% by weight, respectively) that exhibits outstanding properties such as a low melting point ( $-19\text{ }^{\circ}\text{C}$ ), high electrical conductivity ( $3.46 \times 10^6\text{ Sm}^{-1}$ ), a high boiling point ( $1300\text{ }^{\circ}\text{C}$ ), favourable thermal conductivity ( $16.5\text{ W m}^{-1}\text{ K}^{-1}$ ), and an ultra-low vapor pressure which can exist in the liquid phase at room temperature.

### Fabrication of the liquid-metal-based stretchable pulse sensor

Fig. 1 shows the fabrication process for the stretchable pulse sensor using the selective wetting behaviour of a reduced liquid-metal. An optically clear, inert, non-toxic, and non-flammable material known as PDMS was spin-coated on a Si wafer (800 rpm for 30 s) and then placed on a hot plate at  $80\text{ }^{\circ}\text{C}$  for 90 min. After the curing process, the PDMS layer was exposed to oxygen plasma at 60 W for 90 s, which enhances the adhesion ability between the metal and the PDMS. Next, a Au/Cr thin layer was deposited on the sample, and electrical circuits for the pulse sensor were obtained using conventional photolithography and Au/Cr wet-etching processes. Surface cracking occurs with a higher probability when oxygen plasma treatment is done before Cr/Au (10/100 nm) deposition on elastomer substrates.<sup>37,38</sup> This can be minimized by using HMDS (hexamethyldisiloxane) treatment, which is employed to enhance the adhesion ability between the metal and the PDMS layer (shown in Fig. S5 of the ESI†). Before Au/Cr metal deposition, the PDMS layer was placed in HMDS vapor in a sealed environment for 12 hours. Even if surface cracking occurs, it has no influence on the liquid metal pattern. As shown in Fig. S6(a) of the ESI†, there is some surface cracking on the Au patterns when the PDMS layer is treated with oxygen plasma. However, the metal surface cracking disappeared after being covered by a thin Cu layer using an



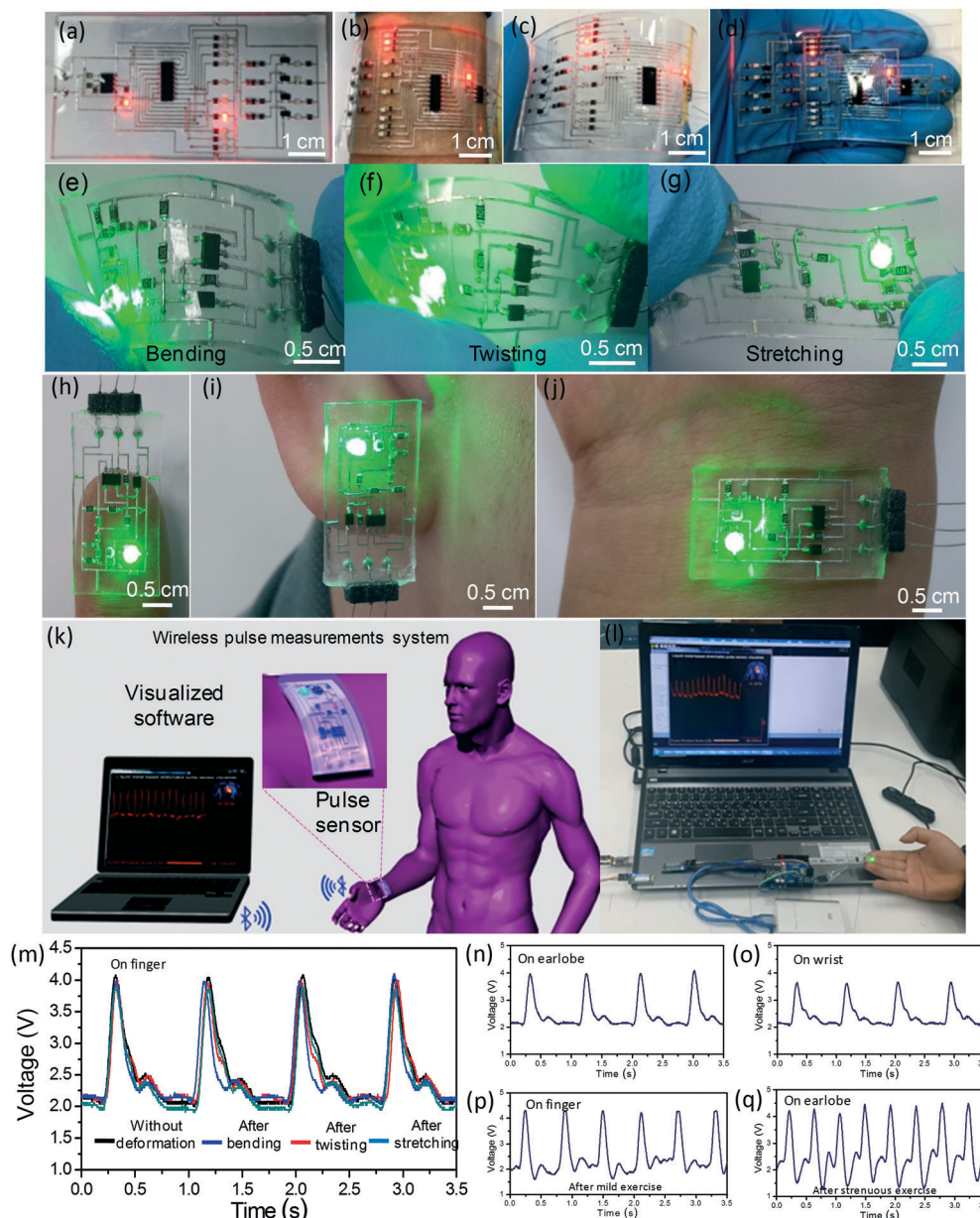


**Fig. 5** A transparent flowing LED light and a liquid-metal-based stretchable pulse sensor; (a) the top view of the transparent flowing LED light working under (b–g) various conditions include bending, twisting, stretching, etc. (h–j) The liquid-metal-based stretchable pulse sensor attached to various parts of the human body (finger, earlobe, and wrist). (k) Sketch of the wireless pulse-measurement system. (l) The wireless pulse-measurement system consists of the liquid-metal-based stretchable pulse sensor, a Bluetooth module, a computer, and a self-programmed visualization software program. (m–q) Measurement results of the human heartbeat under various conditions when attached to parts of the human body.

electroplating technique as shown in Fig. S6(b) of the ESI.<sup>†</sup> Therefore, the surface cracking has no influence on the uniformity of the liquid metal pattern, as shown in Fig. S6(c) of the ESI.<sup>†</sup> This is due to the liquid characteristics of the metallic material. After the wet-etching processes, the Au/Cr patterns were covered by a thin Cu layer using an electroplating technique. The thin metal patterns were then covered again using a liquid-metal droplet treated with a 37 wt% HCl solution. The reduced liquid-metal droplet was rolled over the patterns for 2 min, which ensures that the reduced liquid

metal fully wets the patterned Cu layer. Finally, the remainder of the reduced liquid-metal was removed from the circuits. After rinsing with an acetone solution, the liquid metal circuit pattern was treated with isopropyl alcohol (IPA) and placed on a hot plate at 60 °C for 5 min. The electronic elements (including an optical receiver (APDS-9008), a LED, an operational amplifier chip (MCP6001), diodes, resistors, and capacitors) were then integrated into the liquid metal wires to realize a functional circuit. After integration, the sensor circuit was covered with a PDMS solution and placed on a

hot plate at 60 °C for 4 h. After curing, the Si substrate was removed to release the stretchable sensor embedded in PDMS.

## Conflicts of interest

There are no conflicts to declare.

## Acknowledgements

This study was supported by the National Research Foundation Grant (No. 2015R1A2A2A05001405) and the Commercialization Promotion Agency for R&D Outcomes (COMPA) funded by the Ministry of Science, ICT and Future Planning (MSIP) (No. 2016K000209). It was also partially supported by the China Postdoctoral Science Foundation (No. 2017M611963) and the Talent Planning Project (No. ZX2017000230).

## References

- 1 T. Gao, J. Liao, J. Wang, Y. Qiu, Q. Yang, M. Zhang, Y. Zhao, L. Qin, H. Xue and Z. Xiong, *J. Mater. Chem. A*, 2015, 3, 9965–9971.
- 2 C.-S. Hu, Y.-F. Chung, C.-C. Yeh and C.-H. Luo, *J. Evidence-Based Complementary Altern. Med.*, 2011, 2012, 745127.
- 3 Y. Jiang, H. Hamada, S. Shiono, K. Kanda, T. Fujita, K. Higuchi and K. Maenaka, *Procedia Eng.*, 2010, 5, 1466–1469.
- 4 Y. Wang, L. Wang, T. Yang, X. Li, X. Zang, M. Zhu, K. Wang, D. Wu and H. Zhu, *Adv. Funct. Mater.*, 2014, 24, 4666–4670.
- 5 X. Chen, J. Shao, N. An, X. Li, H. Tian, C. Xu and Y. Ding, *J. Mater. Chem. C*, 2015, 3, 11806–11814.
- 6 C. Pang, J. H. Koo, A. Nguyen, J. M. Caves, M.-G. Kim, A. Chortos, K. Kim, P. J. Wang, J. B.-H. Tok and Z. Bao, *Adv. Mater.*, 2015, 27, 634–640.
- 7 G. Zhu, W. Q. Yang, T. Zhang, Q. Jing, J. Chen, Y. S. Zhou, P. Bai and Z. L. Wang, *Nano Lett.*, 2014, 14, 3208–3213.
- 8 L. Gao, Y. Zhang, V. Malyarchuk, L. Jia, K.-I. Jang, R. C. Webb, H. Fu, Y. Shi, G. Zhou, L. Shi, D. Shah, X. Huan, B. Xu, C. Yu, Y. Huang and J. A. Rogers, *Nat. Commun.*, 2014, 5, 4938.
- 9 M. S. Mannoor, H. Tao, J. D. Clayton, A. Sengupta, D. L. Kaplan, R. R. Naik, N. Verma, F. G. Omenetto and M. C. McAlpine, *Nat. Commun.*, 2012, 3, 763.
- 10 M. D. Dickey, *Adv. Mater.*, 2017, 1606425, 1–19.
- 11 S. Gong, W. Schwalb, Y. Wang, Y. Chen, Y. Tang, J. Si, B. Shirinzadeh and W. Cheng, *Nat. Commun.*, 2014, 5, 1–8.
- 12 A. J. Bandyopadhyay, I. Jeeran, J. You, R. Nuñez-Flores and J. Wang, *Nano Lett.*, 2016, 16, 721–727.
- 13 M. Amjadi, A. Pichitpajongkit, S. Lee, S. Ryu and I. Park, *ACS Nano*, 2014, 8, 5154–5163.
- 14 S. H. Jeong, A. Hagman, K. Hjort, M. Jobs, J. Sundqvist and Z. G. Wu, *Lab Chip*, 2012, 12, 4657–4664.
- 15 S. H. Jeong, K. Hjort and Z. G. Wu, *Sensors*, 2014, 14, 16311–16321.
- 16 S. Cheng and Z. G. Wu, *Lab Chip*, 2010, 10, 3227–3234.
- 17 C. Fassler and C. Majidi, *Smart Mater. Struct.*, 2013, 22, 055023.
- 18 E. Palleau, S. Reece, S. C. Desai, M. E. Smith and M. D. Dickey, *Adv. Mater.*, 2013, 25, 1589–1592.
- 19 K. Khoshmanesh, S. Tang, J. Y. Zhu, S. Schaefer, A. Mitchell, K. Kalantar-zadeh and M. D. Dickey, *Lab Chip*, 2017, 17, 974–993.
- 20 S. Zhu, J.-H. So, R. Mays, S. Desai, W. R. Barnes, B. Pourdeyhimi and M. D. Dickey, *Adv. Funct. Mater.*, 2013, 23, 2308–2314.
- 21 S. H. Jeong, K. Hjort and Z. G. Wu, *Sci. Rep.*, 2015, 5, 08419.
- 22 Q. Zhang, Y. Gao and J. Liu, *Appl. Phys. A: Mater. Sci. Process.*, 2014, 116, 1091–1097.
- 23 L. Wang and J. Liu, *RSC Adv.*, 2015, 5, 57686–57691.
- 24 Y. Gao, H. Li and J. Liu, *PLoS One*, 2012, 7, e45458.
- 25 Y. Zheng, Z. He, Y. Gao and J. Liu, *Sci. Rep.*, 2013, 3, 01786.
- 26 A. Tabatabai, A. Fassler, C. Usiak and C. Majidi, *Langmuir*, 2013, 29, 6194–6200.
- 27 C. Ladd, J. So, J. Muth and M. D. Dickey, *Adv. Mater.*, 2013, 25, 5081–5085.
- 28 J. W. Boley, E. L. White, G. T.-C. Chiu and R. K. Kramer, *Adv. Funct. Mater.*, 2014, 24, 3501–3507.
- 29 Y. Zheng, Z. Z. He, J. Yang and J. Liu, *Sci. Rep.*, 2014, 4, 04588.
- 30 R. K. Kramer, C. Majidi and R. J. Wood, *Adv. Funct. Mater.*, 2013, 23, 5292–5296.
- 31 G. Li, X. Wu and D.-W. Lee, *Lab Chip*, 2016, 16, 1366–1373.
- 32 G. Li, M. Parmar and D.-W. Lee, *2013 13th IEEE Conference on Nanotechnology (IEEE-NANO)*, 2013, pp. 410–413.
- 33 G. Li, M. Parmar, D. Kim, J.-B. Lee and D.-W. Lee, *Lab Chip*, 2014, 14, 200–209.
- 34 G. Li, M. Parmar and D.-W. Lee, *Lab Chip*, 2015, 15, 766–775.
- 35 G. Li, X. Wu and D.-W. Lee, *2015 Transducers - 2015 18th International Conference on Solid-State Sensors, Actuators and Microsystems (TRANSDUCERS)*, 2015, pp. 339–342.
- 36 G. Li, X. Wu and D.-W. Lee, *Sens. Actuators, B*, 2015, 221, 1114–1119.
- 37 O. Graudejus, P. Görrn and S. Wagner, *ACS Appl. Mater. Interfaces*, 2010, 2, 1927–1933.
- 38 C. Huang, J. Lv, X. Tian, Y. Wang, Y. Yu and J. Liu, *Sci. Rep.*, 2015, 5, 14787.